Chapter 12

Advanced Control Techniques for Induction Motors

Manuel A. Duarte-Mermoud and Juan C. Travieso-Torres

Additional information is available at the end of the chapter

http://dx.doi.org/10.5772/50237

1. Introduction

The design of suitable control algorithms for induction motors (IM) has been widely investigated for more than two decades. Since the beginning of field oriented control (FOC) of AC drives, seen as a viable replacement of the traditional DC drives, several techniques from linear control theory have been used in the different control loops of the FOC scheme, such as Proportional Integral (PI) regulators, and exact feedback linearization (Bose, 1997, 2002; Vas, 1998). Due to their linear characteristics, these techniques do not guarantee suitable machine operation for the whole operation range, and do not consider the parameter variations of the motor-load set.

Several nonlinear control techniques have also been proposed to overcome the problems mentioned above, such as sliding mode techniques (Williams & Green, 1991; Al-Nimma & Williams, 1980; Araujo & Freitas, 2000) and artificial intelligence techniques using fuzzy logic, neuronal networks or a combination of them (Vas, 1999; Al-Nimma & Williams, 1980; Bose, 2002). All these techniques are based on complex control strategies differing of the advanced control techniques described here.

In this chapter we present a collection of advanced control strategies for induction motors, developed by the authors during the last ten years, which overcome some of the disadvantages of the previously mentioned control techniques. The techniques studied and presented in this chapter are based on equivalent passivity by adaptive feedback, passivity by interconnection and damping assignment (IDA-PCB) and fractional order proportional-integral controller (FOPIC) in the standard field oriented control scheme (FOC).

All of the control strategies described here guarantee high performance control, such as high starting torque at low speed and during the transient period, accuracy in steady state, a wide range of speed control, and good response under speed and load changes. For all of

the control strategies developed throughout the chapter, after a brief theoretical description of each one of them, simulation as well as experimental results of their application to control IM are presented and discussed.

The main contribution of this Chapter is to show that IM control techniques based on passivity, IDA-PCB and FOPIC can be successfully used in a FOC scheme, presenting some advantages over the classical techniques.

2. Adaptive passivity based control for the IM

Four novel adaptive passivity based control (APBC) techniques were first developed by the main author and his collaborators. As explained in Sections 2.1 and 2.2, these are the adaptive approach of feedback passive equivalence controllers, which were developed for SISO (Castro-Linares & Duarte-Mermoud, 1998; Duarte-Mermoud et al, 2001) and MIMO systems (Duarte-Mermoud et al 2003; Duarte-Mermoud et al, 2002), including controllers with fixed adaptive gains (CFAG) as well as controllers with time-varying adaptive gains (CTVAG). The nonlinear model characteristics were considered in the controller design and they are adaptive in nature, guaranteeing robustness under all model parameter variations.

These techniques were developed for systems parameterized in the so called normal form with explicit linear parametric dependence, which are also locally weakly minimum phase. It can be verified that the IM can be expressed in that particular form and therefore these strategies can be readily applied to them.

Based on the APBC control techniques developed for SISO systems, previously presented, two novel control strategies for induction motors were proposed in Travieso-Torres & Duarte-Mermoud (2008) as described in Section 2.3. Besides, a MIMO version, based on the MIMO techniques already mentioned, was applied to the IM in Duarte-Mermoud & Travieso-Torres (2003) and described here in Section 2.4. Results from SISO and MIMO controllers are similar, however the SISO controllers present only two adjustable parameters by means of simple adaptive laws, being simpler than the solution for the MIMO case, since the MIMO controllers have a larger number of adjustable parameters.

These controllers are applied to the IM considering the scheme presented in Figure 1. In both cases, SISO and MIMO controllers were suitably simplified using the Principle of Torque-Flux Control (PTFC) proposed in Travieso (2002). This principle is applicable to strategies working under a FOC scheme. Based on the PTFC, the design of the SISO and MIMO controllers do not require flux estimations.

For the SISO and the MIMO approaches, the proposed CFAG is simpler, but better transient behaviour was obtained when CTVAG was used. The results were compared with the classical basic control scheme (BCS) shown in Figure 2 (Chee-Mun, 1998), concluding that the proposed adaptive controllers showed a better transient behaviour. In addition, CFAG and CTVAG do not need the knowledge of the set motor–load parameters and robustness under variations of such parameters is guaranteed.

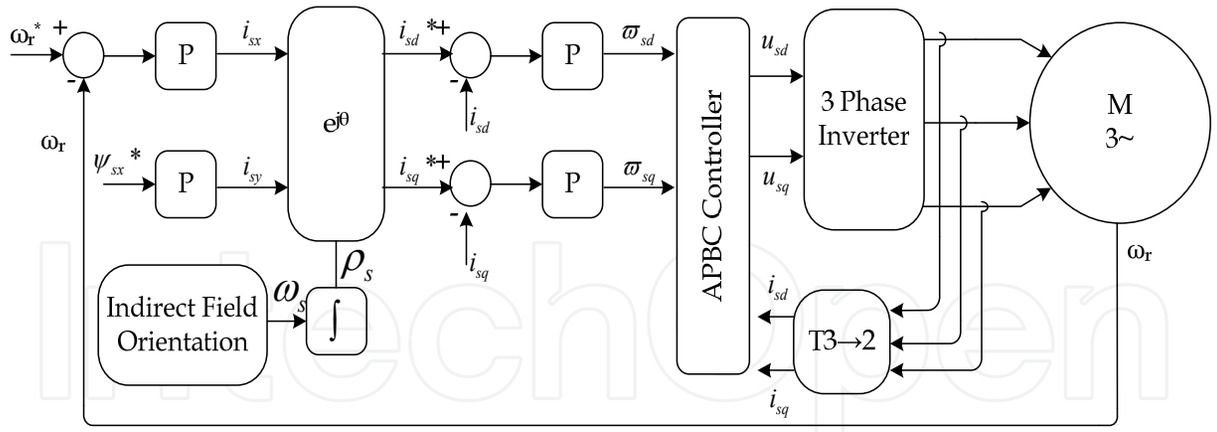

Figure 1. Proposed control scheme with field oriented block (APBC)

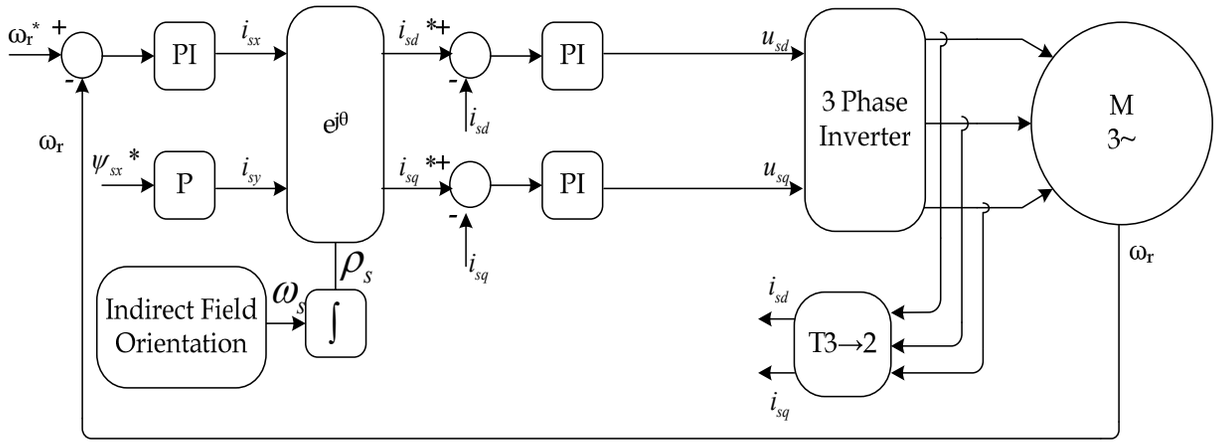

Figure 2. Basic control scheme with field oriented block (BCS)

2.1. SISO Adaptive Passivity Based Control (ABPC) theory

The SISO APBC approach was proposed in Castro-Linares & Duarte-Mermoud (1998) and Duarte-Mermoud et al (2001), for systems parameterized in the following normal form (Byrnes et al, 1991), with explicit linear parametric dependence

$$\begin{aligned} \dot{y} &= \Lambda_a^T A(y,z) + \Lambda_b B(y,z) u \\ \dot{z} &= \Lambda_0 f_o(z) + \Lambda_p P(y,z) y \end{aligned} \tag{1}$$

with $z \in \Re^n$, $y \in \Re$, $u \in \Re$, $A(y, z) \in \Re^m$, $B(y, z) \in \Re$, $f_0 \in \Re^n$, $P(y, z) \in \Re^n$; and the parameters $\Lambda_a \in \Re^m$, $\Lambda_b \in \Re$, $\Lambda_0 \in \Re^{nxn}$, $\Lambda_p \in \Re^{nxn}$. The function $\dot{z} = \Lambda_0 f_0(z)$ is known as zero dynamics (Isidori, 1995; Nijmiejer & Van der Shaft, 1996). Besides, it is necessary to check that the system is locally weakly minimum phase by finding a positive definite differentiable function $W_0(z)$ satisfying $\left(\partial W_0(z)/\partial z\right)^T \Lambda_0 f_0(z) \le 0, \forall \Lambda_0$ (Byrnes et al, 1991). According to the theory presented in the original papers, for locally weakly minimum phase systems of the form (1) with matrix $B(y,z)$ being invertible, there exist two adaptive controllers guaranteeing stability described in the following section.

2.1.1. SISO controller with fixed gains

A SISO controller with fixed adaptive gains (CFAG) was proposed in Castro-Linares & Duarte-Mermoud (1998) for SISO systems of the form (1). This controller has the following form

$$u(y,z,\theta_h)=\frac{1}{B}\left[\theta_1^{\,T}(t)A(y,z)-\theta_2(t)P(y,z)\frac{\partial W_0(z)}{\partial z}+\theta_3(t)\varpi\right] \tag{2}$$

with $z \in \Re^2$, $y \in \Re$, $u \in \Re$, $A(y, z) \in \Re$, $B(y, z) \in \Re$, $f_0 \in \Re^2$, $P(y, z) \in \Re^2$ and the adjustable parameters $\theta_1(t) \in \Re^p$ and $\theta_2(t), \theta_4(t) \in \Re$ updated with the adaptive laws

$$\begin{aligned}\dot{\theta}_1(t)&=-sign(\Lambda_b)A(y,z)y\\ \dot{\theta}_2(t)&=-sign(\Lambda_b)yP(y,z)\left(\frac{\partial W_0(z)}{\partial z}\right)\\ \dot{\theta}_3(t)&=-sign(\Lambda_b)y\varpi\end{aligned} \tag{3}$$

that applied to system (1) make it locally feedback equivalent to a C²-passive system from the new input ϖ to the output y. The parameters $\Lambda_a \in \Re$, $\Lambda_b \in \Re$, $\Lambda_0 \in \Re$, $\Lambda_p \in \Re^{2x2}$ represent constant but unknown parameters from a bounded compact set Ω.

2.1.2. SISO controller with time-varying gains

Another adaptive controller approach but with time-varying gains (Duarte-Mermoud et al, 2001) was also proposed for a SISO system of the form (1). This controller has the same control law shown in (2), but updated with the following adaptive laws

$$\begin{aligned}\dot{\theta}_1(t)&=-sign(\Lambda_b)\left(\gamma_1^{-1}(t)/\sqrt{1+\frac{1}{\gamma(t)^T\gamma(t)}}\right)A(y,z)y\\ \dot{\theta}_2(t)&=-sign(\Lambda_b)\left(\gamma_2^{-1}(t)/\sqrt{1+\frac{1}{\gamma(t)^T\gamma(t)}}\right)P(y,z)\left(\frac{\partial W_0(z)}{\partial z}\right)y\\ \dot{\theta}_3(t)&=-sign(\Lambda_b)\left(\gamma_3^{-1}(t)/\sqrt{1+\frac{1}{\gamma(t)^T\gamma(t)}}\right)\varpi y\end{aligned} \tag{4}$$

where $\gamma_1(t) \in \Re^{4\times4}$ and $\gamma_2(t), \gamma_3(t), \gamma_4(t) \in \Re$ are time-varying adaptive gains defined by

$$\begin{aligned}&\dot{\gamma}_1(t)=-\left[\gamma_1 A(y,z)A^T(y,z)\gamma_1\right],\\ &\dot{\gamma}_2(t)=\left[\gamma_2(t)P(y,z)\left(\frac{\partial W_0(z)}{\partial z}\right)\right]^2, \qquad \gamma(t)=\left[Trace\{\gamma_1(t)\}\quad \gamma_2(t)\quad \gamma_3(t)\right]\in\Re^3\\ &\dot{\gamma}_3(t)=\left[\gamma_3(t)\varpi\right]^2.\end{aligned} \tag{5}$$

2.2. MIMO Adaptive Passivity Based Control (ABPC) theory

The MIMO APBC approach was proposed in Duarte-Mermoud et al (2002) and Duarte-Mermoud et al (2003), for systems parameterized in the following normal form (Byrne et al, 1991), with explicit linear parametric dependence

$$\begin{aligned} \dot{y} &= \Lambda_a A(y,z) + \Lambda_b B(y,z)u \\ \dot{z} &= \Lambda_0 f_0(z) + P^T(y,z)\Lambda_p y \end{aligned} \tag{6}$$

with $z \in \Re^2$, $y \in \Re^2$, $u \in \Re^2$, $A(y,z) \in \Re^8$, $B(y,z) \in \Re^{2x2}$, $f_0 \in \Re^2$, $P(y,z) \in \Re^{2x2}$. The parameters $\Lambda_a \in \Re^{2x8}$, $\Lambda_b \in \Re^{2x2}$, $\Lambda_0 \in \Re^{2x2}$ and $\Lambda_p \in \Re^{2x2}$ represent constant but unknown parameters from a bounded compact set Ω. The term $\dot{z} = \Lambda_0 f_0(z)$ is the so called zero dynamics (Isidori, 1995; Nijmiejer & Van der Shaft, 1996). In this case it is also necessary to check that system (6) is locally weakly minimum phase by finding a positive definite differentiable function $W_0(z)$ satisfying $\left(\partial W_0(z)/\partial z\right)^T \Lambda_0 f_0(z) \le 0, \forall \Lambda_0$ (Byrnes et al, 1991). According to the theory presented in the original papers, for locally weakly minimum phase systems of the form (11) with matrix $B(y,z)$ being invertible, there exist two type of adaptive controllers guaranteeing stability which are described in the following section.

2.2.1. MIMO controller with fixed gains

According to Duarte-Mermoud et al (2002) there exists an adaptive controller of the form

$$u(t) = \left[\theta_1(t)A(y,z) - \theta_2(t)P(y,z)\frac{\partial W_0(z)}{\partial z} + \theta_3(t)\varpi(t) \right] \tag{7}$$

with the adaptive laws

$$\begin{aligned} \dot{\theta}_1(t) &= -yA^T(y,z) \\ \dot{\theta}_2(t) &= -y\left(\frac{\partial W_0(z)}{\partial z}\right)^T P^T(y,z) \\ \dot{\theta}_3(t) &= -y\varpi^T(t) \end{aligned} \tag{8}$$

that applied to system (6) make it locally feedback equivalent to a C^2-passive system from the input $\varpi(t)$ to the output $y(t)$. The parameters $\theta_1(t) \in \Re^{2x8}$, $\theta_2(t) \in \Re^{2x2}$ and $\theta_3(t) \in \Re^{2x2}$ represent adjustable controller parameters whose ideal values are $\theta^*_1 = -\Lambda_b^{-1}\Lambda_a \in \Re^{2x8}$, $\theta^*_2 = -\Lambda_b^{-1}\Lambda_p^T \in \Re^{2x2}$ and $\theta^*_3 = \Lambda_b^{-1} \in \Re^{2x2}$.

2.2.2. MIMO controller with time-varying gains

On the other hand, CTVAG was proposed in Duarte-Mermoud et al (2003). This controller has the same form (7), but with adaptive laws given by

$$\dot{\theta}_1(t) = -yA^T(y,z)\frac{\Gamma_1^{-1}}{\sqrt{1+Trace\left(\Gamma_1^{-2}+\Gamma_2^{-2}+\Gamma_3^{-2}\right)}}$$

$$\dot{\theta}_2(t) = -\frac{\Gamma_2^{-1}}{\sqrt{1+Trace\left(\Gamma_1^{-2}+\Gamma_2^{-2}+\Gamma_3^{-2}\right)}} y\left(\frac{\partial W_0(z)}{\partial z_1}\right)^T P^T(y,z) \tag{9}$$

$$\dot{\theta}_3(t) = -\frac{\Gamma_3^{-1}}{\sqrt{1+Trace\left(\Gamma_1^{-2}+\Gamma_2^{-2}+\Gamma_3^{-2}\right)}} y\varpi^T(t)$$

and time-varying adaptive gains defined by

$$\begin{aligned}
&\dot{\Gamma}_1 = -\Gamma_1 A(y,z)A^T(y,z)\Gamma_1, && \Gamma_1(t_0) > 0\\
&\dot{\Gamma}_2 = -\Gamma_2 P(y,z)\left(\frac{\partial W_0(z)}{\partial z}\right)\left(\frac{\partial W_0(z)}{\partial z}\right)^T P^T(y,z)\Gamma_2, && \Gamma_2(t_0) > 0\\
&\dot{\Gamma}_3 = -\Gamma_3 \varpi(t)\varpi^T(t)\Gamma_3, && \Gamma_3(t_0) > 0
\end{aligned} \tag{10}$$

According to Duarte-Mermoud et al (2002), this controller applied to system (6) will convert it to an equivalent C²-passive system from the input $\varpi(t)$ to the output $y(t)$. The parameters $\theta_1(t) \in \Re^{2x8}$, $\theta_2(t) \in \Re^{2x2}$ and $\theta_3(t) \in \Re^{2x2}$ represent adjustable controller parameters whose ideal values are $\theta^*_1 = -\Lambda_b^{-1}\Lambda_a \in \Re^{2x8}$, $\theta^*_2 = -\Lambda_b^{-1}\Lambda_p^T \in \Re^{2x2}$ and $\theta^*_3 = \Lambda_b^{-1} \in \Re^{2x2}$

2.3. SISO ABPC applied to the IM

In this Section the design of SISO CFAG and SISO CTVAG for IM is explained, based on the SISO theories previously described.

2.3.1. SISO IM modeling

In order to apply the controllers described in Section 2.1 the IM model was expressed as SISO subsystems parameterized in the following locally weakly minimum phase normal form with explicit linear parametric dependence. For Subsystem 1 we have

$$\Lambda_{a1} = \begin{bmatrix} -\frac{R'_s}{\sigma L_s} & 1 & \frac{L_m R_r}{\sigma L_s L_r^2} & \frac{L_m}{\sigma L_s L_r} \end{bmatrix}^T, \quad A_1(y_i,z) = \begin{bmatrix} e_{i_{sx}} \\ \omega_g e_{i_{sy}} \\ e_{\psi_{rx}} \\ \omega_r e_{\psi_{ry}} \end{bmatrix}, \quad \Lambda_{b1} = \frac{1}{\sigma L_s}, \quad B_1(y_i,z) = 1,$$

$$\Lambda_{p1} = \begin{bmatrix} \frac{L_m}{T_r} & 0 \\ 0 & \frac{L_m}{T_r} \end{bmatrix}, \quad y_1 = e_{i_{sx}}, \quad P_1(y_i,z) = \begin{bmatrix} P_{11} \\ P_{21} \end{bmatrix} = \begin{bmatrix} 1 \\ \frac{\dot{e}_{i_{sy}}}{\dot{e}_{i_{sx}}} \end{bmatrix}, \quad u_1 = e_{u_{sx}}. \tag{11}$$

For Subsystem 2 we can write

$$\Lambda_{a2}=\begin{bmatrix}-\dfrac{R'_s}{\sigma L_s} & -1 & \dfrac{L_m R_r}{\sigma L_s L_r^2} & -\dfrac{L_m}{\sigma L_s L_r}\end{bmatrix}^T,\quad A_2(y_i,z)=\begin{bmatrix}e_{i_{sy}}\\ \omega_g e_{i_{sx}}\\ e_{\psi_{ry}}\\ \omega_r e_{\psi_{rx}}\end{bmatrix},\quad \Lambda_{b2}=\frac{1}{\sigma L_s},\quad B_2(y_i,z)=1,$$
$$\Lambda_{p2}=\begin{bmatrix}\dfrac{L_m}{T_r} & 0\\ 0 & \dfrac{L_m}{T_r}\end{bmatrix},\quad y_2=e_{i_{sy}},\quad P_2(y_i,z)=\begin{bmatrix}P_{12}\\ P_{22}\end{bmatrix}=\begin{bmatrix}\dfrac{\dot{e}_{i_{sx}}}{\dot{e}_{i_{sy}}}\\ 1\end{bmatrix},\quad u_2=e_{u_{sy}}. \tag{12}$$

2.3.2. Principle of torque – Flux control

The PTFC, proposed in Travieso (2002), states that in controlling the torque and flux for IM, the controllers design can be focused only to control the stator currents. This is true for the case when a scheme with coordinate transformation block $e^{j\rho_g}$ (Field Oriented Scheme), to transform from a stationary to a rotating coordinate system, is considered. Therefore, it is pointless to make efforts to directly control rotor flux or rotor current components. It is proven in Travieso (2002) that the controller still guarantees suitable control of the torque and flux and making it possible to discard all the terms concerning the rotor current or rotor flux components in its design.

2.3.3. SISO CFAG applied to the IM

In Travieso-Torres & Duarte-Mermoud (2008) a simplified controller for IM was proposed based on the theories from Castro-Linares & Duarte-Mermoud (1998). After applying the PTFC and considering the controller directly feeding the IM in the stator coordinate system, this means that ωg = 0, this SISO controller has the following form

$$\left.\begin{aligned}u_i(y_i,z,\theta_{hi})&=\theta_{1i}y_i+\theta_{4i}\varpi_i\\ \dot{\theta}_{1i}&=-y_i^2\\ \dot{\theta}_{4i}&=-y_i\varpi_i\end{aligned}\right\}\quad\begin{matrix}i=1,2\\ h=1,4\end{matrix} \tag{13}$$

2.3.4. SISO CTVAG applied to the IM

Another adaptive controller but with time-varying gains was also proposed in Travieso-Torres & Duarte-Mermoud (2008), based on the results of Duarte-Mermoud & Castro-Linares (2001). This controller, after applying the PTFC and considering the controller directly feeding the motor in the stator coordinate system, has the following form

$$\left.\begin{aligned} u_i(y_i,z,\theta_{hi}) &= \theta_{1i}y_i + \theta_{4i}\varpi_i \\ \dot{\theta}_{1i} &= -sign(\Lambda_{bi}^*)\left(\gamma_1^{-1}/\sqrt{1+\frac{1}{\gamma_i^T\gamma_i}}\right)y_i^2, \\ \dot{\theta}_{4i} &= -sign(\Lambda_{bi}^*)\left(\gamma_4^{-1}/\sqrt{1+\frac{1}{\gamma_i^T\gamma_i}}\right)\varpi_i y_i, \end{aligned}\right\} \text{with} \quad \begin{aligned} \dot{\gamma}_{1i} &= -\left(\gamma_{1i}y_i\right)^2 \\ \dot{\gamma}_{4i} &= -\left(\gamma_{4i}\varpi_i\right)^2 \end{aligned} \quad \text{and} \quad \begin{aligned} i &= 1,2 \\ h &= 1,4 \end{aligned} \tag{14}$$

2.4. MIMO ABPC applied to the IM

In this Section the design of the MIMO CFAG and the MIMO CTVAG for the IM are presented, based on the MIMO theories previously stated.

2.4.1. MIMO model of the IM

In order to apply controllers from Duarte-Mermoud et al (2002) and Duarte-Mermoud et al (2003), the IM model was expressed in form (6) as follows

$$\dot{y} = \begin{bmatrix} -\frac{R'_s}{\sigma L_s} & 0 & 0 & 1 & \frac{L_m R_r}{\sigma L_s L_r^2} & 0 & 0 & -\frac{L_m}{\sigma L_s L_r} \\ 0 & -\frac{R'_s}{\sigma L_s} & -1 & 0 & 0 & \frac{L_m R_r}{\sigma L_s L_r^2} & \frac{L_m}{\sigma L_s L_r} & 0 \end{bmatrix} \begin{bmatrix} e_{i_{sx}} \\ e_{i_{sy}} \\ \omega_g e_{i_{sx}} \\ \omega_g e_{i_{sy}} \\ e_{\psi_{rx}} \\ e_{\psi_{ry}} \\ \omega_r e_{\psi_{rx}} \\ \omega_r e_{\psi_{ry}} \end{bmatrix} + \begin{bmatrix} \frac{1}{\sigma L_s} & 0 \\ 0 & \frac{1}{\sigma L_s} \end{bmatrix} I_2 u,$$

$$\dot{z} = \begin{bmatrix} -\frac{R_r}{L_r} & \left(\omega_g - \omega_r\right) \\ -\left(\omega_g - \omega_r\right) & -\frac{R_r}{L_r} \end{bmatrix} \begin{bmatrix} e_{\psi_{rx}} \\ e_{\psi_{ry}} \end{bmatrix} + I_2 \begin{bmatrix} \frac{L_m}{T_r} & 0 \\ 0 & \frac{L_m}{T_r} \end{bmatrix} y, \tag{15}$$

$$\text{with} \quad z = \begin{bmatrix} e_{\psi_{rx}} \\ e_{\psi_{ry}} \end{bmatrix}, \quad y = \begin{bmatrix} e_{i_{sx}} \\ e_{i_{sy}} \end{bmatrix}, \quad u = \begin{bmatrix} e_{u_{sx}} \\ e_{u_{sy}} \end{bmatrix}$$

with $T_r = L_r/R_r$

2.4.2 MIMO CFAG applied to the IM

According to Duarte-Mermoud and Travieso-Torres (2003) there exist an adaptive controller of the form

$$
\begin{aligned}
u(t) &= \theta_1(t) y^T + \theta_3(t)\varpi(t) \\
\dot{\theta}_1(t) &= -yy^T \\
\dot{\theta}_3(t) &= -y\varpi^T(t)
\end{aligned}
\tag{16}
$$

that applied to system (6) makes it locally feedback equivalent to a C²-passive system from the input $\varpi(t)$ to the output $y(t)$. The parameters $\theta_1(t) \in \Re^{2x8}$, $\theta_2(t) \in \Re^{2x2}$ and $\theta_3(t) \in \Re^{2x2}$ represent adjustable controller parameters whose ideal values are $\theta^*_1 = -\Lambda_b^{-1}\Lambda_a \in \Re^{2x8}$, $\theta^*_2 = -\Lambda_b^{-1}\Lambda_p^T \in \Re^{2x2}$ and $\theta^*_3 = \Lambda_b^{-1} \in \Re^{2x2}$.

2.4.3. MIMO CTVAG applied to the IM

Finally a CTVAG was proposed in Duarte-Mermoud and Travieso-Torres (2003). This controller has the following form

$$
\begin{aligned}
&u(t) = \theta_1(t) y + \theta_3(t)\varpi(t) \\
&\dot{\theta}_1(t) = -\left(\Gamma_1^{-1} / \sqrt{1 + Trace\left(\Gamma_1^{-2} + \Gamma_3^{-2}\right)} \right) yy^T, \qquad \dot{\Gamma}_1 = -\Gamma_1 yy^T \Gamma_1, \qquad \Gamma_1(t_0) > 0 \\
&\dot{\theta}_3(t) = -\left(\Gamma_3^{-1} / \sqrt{1 + Trace\left(\Gamma_1^{-2} + \Gamma_3^{-2}\right)} \right) y\varpi^T(t), \qquad \dot{\Gamma}_3 = -\Gamma_3 \varpi(t)\varpi^T(t)\Gamma_3, \qquad \Gamma_3(t_0) > 0
\end{aligned}
\tag{17}
$$

This controller will convert system (6) to an equivalent C²-passive system from the input $\varpi(t)$ to the output $y(t)$. The parameters $\theta_1(t) \in \Re^{2x8}$ and $\theta_3(t) \in \Re^{2x2}$ represent adjustable controller parameters whose ideal values are $\theta^*_1 = -\Lambda_b^{-1}\Lambda_a \in \Re^{2x8}$ and $\theta^*_3 = \Lambda_b^{-1} \in \Re^{2x2}$.

2.5. Simulation results of APBC for the IM

In order to verify the advantages of the proposed controllers a comparison with a traditional current regulated PWM induction motor drive from Chee-Mun (1998) with PI loop controllers (see Figure 2), was carried out. In the simulations a squirrel-cage induction motor whose nominal parameters are: 15 [kW] (20 [HP), 220 [V], fp= 0.853, 4 poles, 60 [Hz], R_s = 0.1062 [Ω], X_{ls}=X_{lr} = 0.2145 [Ω], x_m = 5.8339 [Ω], R_r = 0.0764 [Ω], J = 2.8 [kg m²] and B_p = 0 were considered (Chee-Mun, 1998). All the simulations were made using the software package SIMULINK/MATLAB with ODE 15s (stiff/NDF) integration method and a variable step size.

The obtained control schemes only need the exact values or the estimates of parameters Xm and T_r for the field orientation block. No other parameters or state estimations are used. The PI speed controller is tuned as P=30 and I= 10 according to Chee-Mun (1998).

Figure 3 shows the information used to compare both control schemes. The variations of the reference speed ω^*_r (Figure 3(a)), the variations in load torque (Figure 3(b)), the variation of about 30% in the stator and rotor resistance (Figure 3(c) and Figure 3(d)), the linear increase up to double the load inertia during the motor operation (Figure 3(e)) and the variations in the viscous friction coefficient (Figure 3(f)). For both proposed control strategies (CFAG and

CTVAG) and the classical FOC control (BCS), five comparative tests considering the variations shown in Figure 3 were carried out.

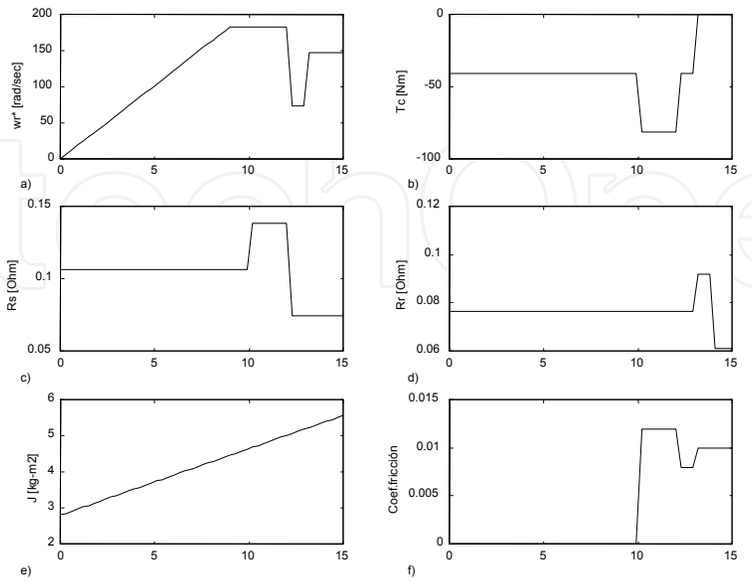

Figure 3. Parameter and reference variations used in the set of comparative tests

These tests allow us to study the behavior of the schemes under the situations described next.

- ***Test 1:*** The reference of speed is increased as a ramp from 0 to 190 [RPM] in 0.5 [s] and the load torque is fixed at the nominal value 69.5 [Nm].
- ***Test 2:*** Variations on load torque, as indicated in Figure 3(b).
- ***Test 3:***Variations on speed reference, as shown in Figure 3(a).
- ***Test 4:*** Variation of the motor resistances, as shown in Figures 3(c) and 3(d).
- ***Test 5:*** Variation of the load parameters, as indicated in Figures 2(e) and 2(f).
- ***Test 6:*** Changes in the controller parameters (P and I) of the control loops.

In all the simulation results of the proposed controllers shown in Figure 4 through 9, the initial conditions of all the controller parameters and adaptive gains were set equal to zero, that is to say, $\theta_{ik}(0) = \gamma_{ih}(0) = 0$, for *i=1,2* y *h=1,4*.

Figure 4 shows the comparative results obtained for the proposed controllers under normal conditions (i.e. according to Test 1), without considering variations of any type. APBC controllers present better transient behavior than traditional PI controllers. CFAG presents a quite accurate stationary state (with a velocity error less than 0.5 %). And CTVAG is equally accurate as the CFAG, but with better transient behavior.

Let us observe next in Figure 5, how the different schemes behave under variations of the load torque, as described in Figure 3(b). In the case of the CFAG shown, the error values are 0.5 % for a nominal load torque and of 0.22% for a half nominal load torque. The **CTVAG** presents a similar response to that of CFAG, but the transient response is slightly better. APBC controllers have better transient behavior than BCS.

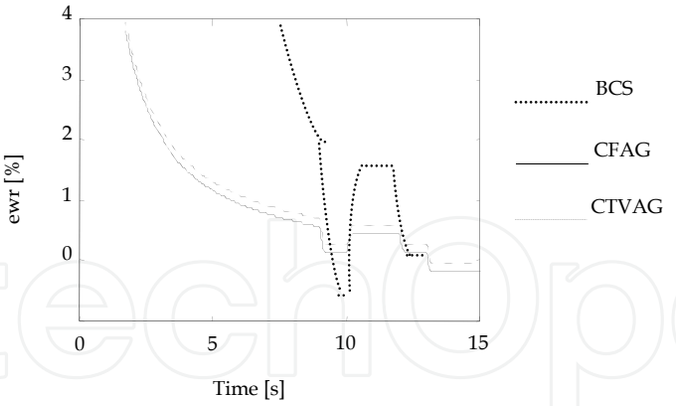

Figure 4. Results for the initial situation

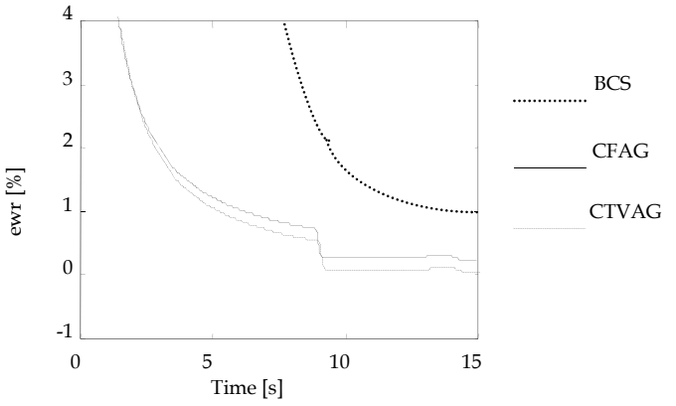

Figure 5. Results under load torque variations

In Figure 6, the effects of speed reference variations at nominal load torque, according to the variations indicated in Figure 3, are presented. The results for the proposed CFAG and CTVAG are similar rendering similar velocity errors whereas the rest of the variables present a suitable behavior. In these cases we have an error of about 0.5 % for nominal speed and of approximately 1.1 % at half the nominal speed.

When analyzing Test 4 (Figures 3(c) and 3(d)) both controllers present good behavior under changes on the stator resistance (see Figure 7). Nevertheless, under changes of the rotor resistance the field orientation is lost and the speed response is affected considerably. Notice how the flow of the machine diminishes considerably when the rotor resistance is decreased. We can also claim that the response in both cases (CFAG and CTVAG)is much more robust than the traditional PI controller of BCS. Both controllers present lesser speed errors in steady state than the classical PI scheme.

Considering now the variations of the load parameters according to Test 5 (Figures 3(e) and 3(f)), neither of the two controllers under study were affected, as is shown in Figure 8. For the proposed controllers, the differences found in the general behavior still remain. CFAG presents a similar error in the steady state than the CTVAG, but with slightly better transient behavior.

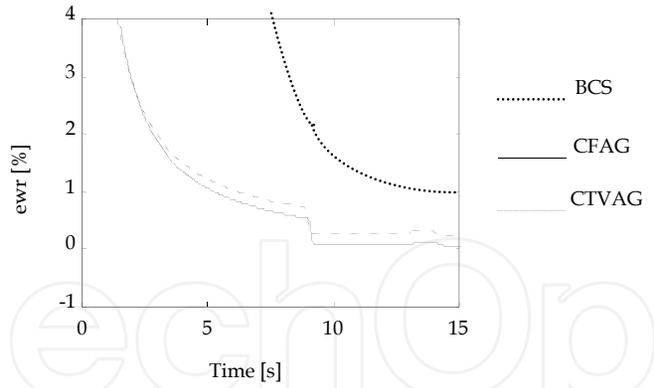

Figure 6. Results for speed reference variations

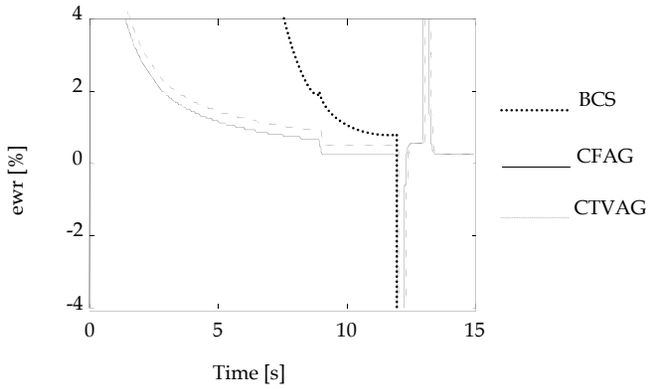

Figure 7. Results for Test 4.

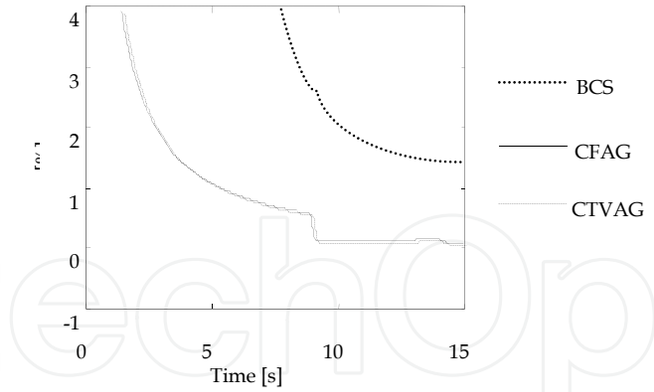

Figure 8. Results under for variations of load parameters

In Figure 9, the proportional gains of all control loops were changed. For CFAG and CTVAG, variations for the speed loop control parameter of 37.5 % were applied (P varies from 80 to 50). The flux loop was varied by 13 %, (P changes from 69 to 60). The current loops were varied by 33.3 % (P varies from 30 to 20). In Figure 9 it can be seen how in spite of these simultaneous gain variations, the speed error continues being less than 1% and the transient response after 0.5 sec. was practically not affected. CFAG as well as CTVAG guarantees good results for a wide range of variations of the proportional gains.

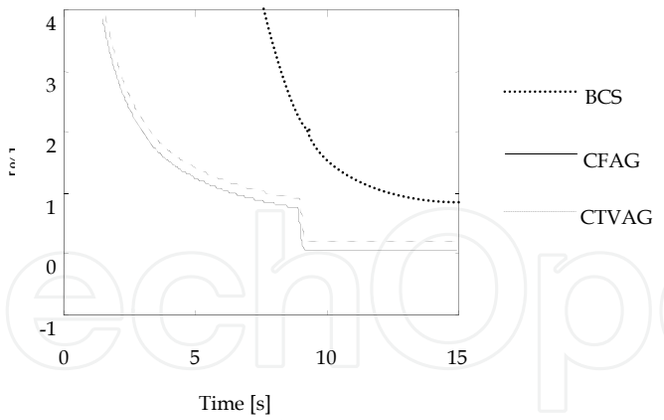

Figure 9. Results under changes in the tuning of the proportional gains

3. Control of IM using IDA-PCB techniques

In this section we will present a brief summary of the *Interconnection and Damping Assignment – Passivity-Based Control (IDA-PBC)* technique and the main ideas on which this method is based. This method provides a novel technique for computing the control necessary for modifying the storage function of a dynamical system assigning a new internal topology (in terms of interconnections and energy dissipation). Further details on the method can be found in Ortega et al. (2002) and Ortega & García-Canseco (2004). Next we will apply this technique to the control of an IM and compare it with BCS and APBC already described in Section 2.

3.1. Foundations of IDA-PCB control

Let us consider a system described in the form called Port-Controlled Hamiltonian (PCH) (Van der Shaft, 2000)

$$\Sigma_{PCH}: \begin{cases} \dot{x} = \left[J(x) - R(x) \right] \nabla H + g(x) u \\ y = g^T(x) \nabla H \end{cases} \tag{18}$$

where $x \in \Re^n$ is the state, and $u, y \in \Re$ are the input and the output of the system. H represents the system's total stored energy, $J(x)$ is a skew-symmetric matrix ($J(x) = -J^T(x)$) called *Interconnection Matrix* and $R(x)$ is a symmetric positive definite matrix ($R(x) = R(x)^T \geq 0$) called *Damping Matrix*. Let us assume (Ortega et al., 2002; Ortega & García-Canseco, 2004) that there exist matrices $g^{\perp}(x)$, $J_d(x) = -J_d{}^T(x)$, $R_d(x) = R_d{}^T(x) \geq 0$ and a function $H_d : \Re^n \to \Re$, such that

$$g^{\perp}(x)\left[J(x) - R(x) \right] \nabla H = g^{\perp}(x)\left[J_d(x) - R_d(x) \right] \nabla H_d \tag{19}$$

where $g^{\perp}(x)$ is the full-rank left annihilator of $g(x)$ ($g^{\perp}(x) g(x) = 0$) and $H_d(x)$ is such that $x^* = \arg\min_{x \in \Re^n} (H_d)$. Then, applying the control $\beta(x)$ defined as

$$\beta(x)=\left[g^T(x)g(x)\right]^{-1}g^T\left\{\left[J_d(x)-R_d(x)\right]\nabla H_d-\left[J(x)-R(x)\right]\nabla H\right\} \tag{20}$$

the overall system under control can be written as

$$\dot{x}=\left[J_d(x)-R_d(x)\right]\nabla H_d \tag{21}$$

where x^* is a locally Lyapunov stable equilibrium. That is to say applying control (20) to (18) the dynamic of the system is changed to that shown in (21). x^* is a locally Lyapunov asymptotically stable equilibrium if it is an isolated minimum of H_d and the largest invariant inside the set $\left\{x\in R^n \middle| \nabla H_d^T(x)R_d(x)\nabla H_d(x)\right\}$ is equal to $\{x^*\}$.

There are two ways to find control (20). The first one consists of fixing the topology of the system (by fixing J_d, R_d and $g^{\perp}$) and solving the differential equation (19). The second method consists of fixing H_d (the initial geometrical form of the desired energy) and then (19) becomes an algebraic system that has to be solved for J_d, R_d and $g^{\perp}$ (Ortega et al., 2002; Ortega & García-Canseco, 2004).

For the IDA-PBC scheme developed in Section 3.2, the model of the IM should be expressed in the PCH form previously stated, which has the general form shown in (18). In this study the load torque will be assumed proportional to rotor speed ($T_c=B\omega_r$) which typically represents fan load type. In this particular case the PCH model of the induction motor (see (22)), assuming also that the speed of the *x-y* reference system is synchronized to electrical frequency ($\omega_s=\omega_s$), has the form (González, 2005, González& Duarte-Mermoud, 2005; González et al., 2008)

$$\begin{aligned}
\dot{x}&=\begin{bmatrix}-R_s & 0 & 0 & 0 & 0\\ 0 & -R_r & 0 & 0 & -x_4\\ 0 & 0 & -R_s & 0 & 0\\ 0 & 0 & 0 & -R_r & x_2\\ 0 & x_4 & 0 & -x_2 & -B'\end{bmatrix}\nabla H+\begin{bmatrix}1 & 0 & x_3\\ 0 & 0 & x_4\\ 0 & 1 & -x_1\\ 0 & 0 & -x_2\\ 0 & 0 & 0\end{bmatrix}\begin{pmatrix}u_{sx}\\ u_{sy}\\ \omega_s\end{pmatrix},\\
y&=\begin{bmatrix}1 & 0 & 0 & 0 & 0\\ 0 & 0 & 1 & 0 & 0\\ x_3 & x_4 & -x_1 & -x_2 & 0\end{bmatrix}\nabla H=\begin{bmatrix}i_{sx}\\ i_{sy}\\ 0\end{bmatrix}\\
x&=\begin{bmatrix}\psi_{sx} & \psi_{rx} & \psi_{sy} & \psi_{ry} & J\omega_r\end{bmatrix}^T=\begin{bmatrix}x_{12}{}^T & x_{34}{}^T & x_5\end{bmatrix}^T,\\
H&=\frac{1}{2}x_{12}{}^TL^{-1}x_{12}+\frac{1}{2}x_{34}{}^TL^{-1}x_{34}+\frac{1}{2}J^{-1}x_5{}^2\\
u&=\begin{bmatrix}u_{sx} & u_{sy} & \omega_s\end{bmatrix}^T, \qquad y=\begin{bmatrix}i_{sx} & i_{sy} & 0\end{bmatrix}^T,\\
&with \qquad L=\begin{bmatrix}L_s & L_m\\ L_m & L_r\end{bmatrix}
\end{aligned} \tag{22}$$

where $\psi_{sx}, \psi_{sy}, \psi_{rx}, \psi_{ry}$ are the stator and rotor fluxes, respectively, and $B' = B_p + B$. In general, when using PCH representation, the obtained state variables are not necessarily the best choice for analysis and additional measurement/estimation may be needed in the controller implementation. Other types of load torque may also be considered in this analysis (e.g. constant, proportional to squared speed, etc.), in which case a slightly different PCH model will be obtained.

3.2. IDA-PBC strategy applied to the IM

The IDA-PBC strategy (Ortega et al., 2002; Ortega & García-Canseco, 2004) consists basically of assigning a new storage function to the closed-loop system, changing the topology of the system, in terms of interconnections and energy transfers between states. In the case of IM (González, 2005, González& Duarte-Mermoud, 2005; González et al., 2008), the controller is defined by some feasible solution for k_1, k_2 and k_3 of the following algebraic equation

$$L^{-1}x_{12} + \left(\begin{array}{c} k_1 \\ \dfrac{x_4}{{x_2}^2 + {x_4}^2} k_3 \end{array} \right) = 0, \quad L^{-1}x_{34} + \left(\begin{array}{c} k_2 \\ \dfrac{x_4}{{x_2}^2 + {x_4}^2} k_3 \end{array} \right) = 0, \quad J^{-1}x_5 + k_3 = 0 \tag{23}$$

From the third equation in (23), it is observed that an equilibrium point $x_5^* = {\omega_r}^*$ exists for ω_r defined as ${\omega_r}^* = -k_3$. For the other parameters (k_1, k_2) the solutions are given by the following relationship $(k_1^2 + k_2^2){L_m}^2 \geq 2k_3 L_r B$ (González, 2005; González et al., 2008).
With the previous results, according to (20), the IDA-PBC controller is defined as

$$\begin{aligned} u_{sx}(x) &= -R_s k_1 + \left(1 + \frac{R_r B'}{{x_2}^2 + {x_4}^2} \right) x_3 k_3, \\ u_{sy}(x) &= -R_s k_2 - \left(1 + \frac{R_r B'}{{x_2}^2 + {x_4}^2} \right) x_3 k_3, \\ \omega_s(x) &= -\left(1 + \frac{R_r B'}{{x_2}^2 + {x_4}^2} \right) k_3 \end{aligned} \tag{24}$$

States x_2 and x_4 correspond to rotor flux expressed in orthogonal coordinates (ψ_{rx}, ψ_{ry}). The rotor flux will be zero if and only if the motor is at rest and without voltage applied. At t=0, some tension has to be applied to control the motor and therefore ψ_r becomes different from zero at t=0. Thus, no undetermined values of the controller are obtained.

The IDA-PBC scheme used in this paper was slightly modified. In principle, this strategy was developed to control the motor speed, not being robust with respect to load perturbations on the motor axis. This means that permanent errors in the mechanical speed were obtained. In order to solve this problem, a simple proportional integral loop was added for the speed error loop modifying the original IDA-PBC, scheme as is shown in Figure 10.

In general the rotor flux cannot be measured in the majority of IM's, which is why it was necessary to implement a rotor flux observer for the experimental implementation of this strategy. The observer was implemented based on the voltage-current model of the induction motor, developed in Marino et al (1994), Jansen et al (1995) and Martin (2005).

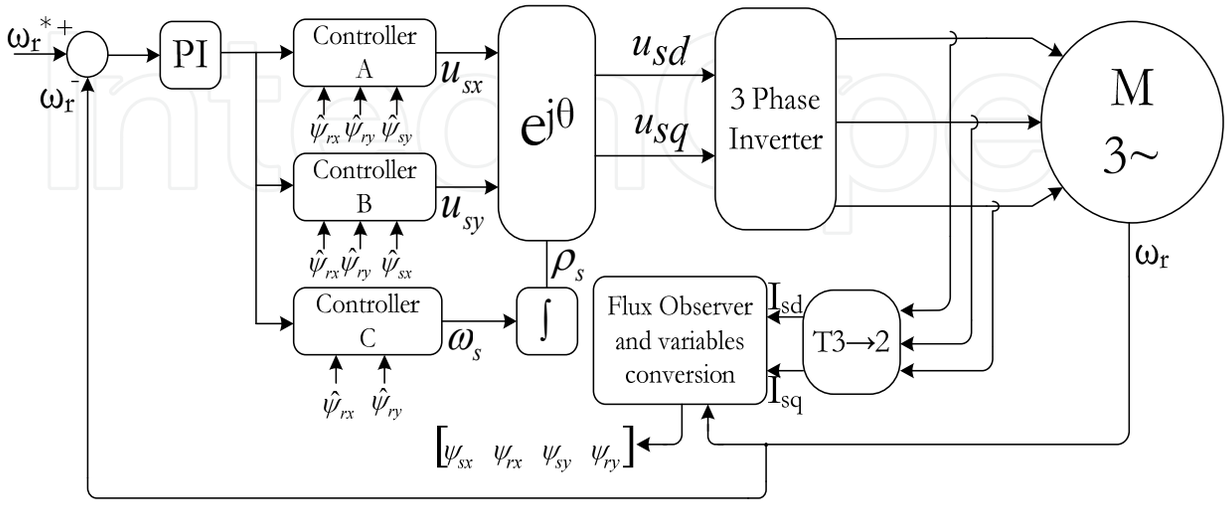

Figure 10. The IDA-PBC control scheme

3.3. Simulation results using IDA-PCB

In this section we present simulation results of applying the IDA-PBC technique for the speed control of an IM (Pelisssier, 2006; Pelisssier & Duarte-Mermoud, 2007). These results are compared with the basic control strategy (BCS) described in Figure 2 and with APBC strategies with fixed and time varying adaptive gains described in Section 2 (Figure 1). The results were obtained using Matlab/Simulink and the IM considered is that described in Chee-Mun (1998). The following two tests were performed on the simulated IM.

Test 1 (Regulation): Speed ramp from zero to nominal speed in 20 seconds with load torque proportional to speed, staring from zero. Then in t=25[s] a load torque of 50% magnitude of the nominal torque value is applied; in t=40[s] the magnitude of the load torque is increased to 100%; in t=60[s] the magnitude of the load torque is decreased to 50% and finally in t=120[s] the load torque is set to zero.

Test 2 (Tracking): Speed ramp from zero to nominal speed in 20 seconds with load torque proportional to speed, staring from zero. Between t=50[s] and 100[s] a pulse train of amplitude $0.1\omega_{r_{nom}}$ and frequency 2π/20 is added to the constant speed reference. Between t=120[s] and 160[s] a sinusoidal speed reference of amplitude $0.1\omega_{r_{nom}}$ and frequency 2π/20 is added to the constant nominal speed reference. The load torque is kept constant in 50% of the nominal torque during the whole test.

The PI controller parameters were first determined using the Ziegler-Nichols criteria and modified later by simulations, until a good response was obtained. For the APB scheme the controllers 'constants were chosen as follows: K_P=0.3 and K_I=0.1 for the external loop and

K_P=500*76.82 for the internal loop. For the IDA-PBC scheme, the values of the parameters were chosen so that equation (23) is satisfied. The values found were k_1=k_2=-7. For the external loop the values were chosen as K_p=K_i=0.5. The results were compared with the BCS described in Figure 2 and the APBC shown in Figure 1.

The simulations results obtained for Test 1 and Test 2 are shown in Figures 11 and 12.

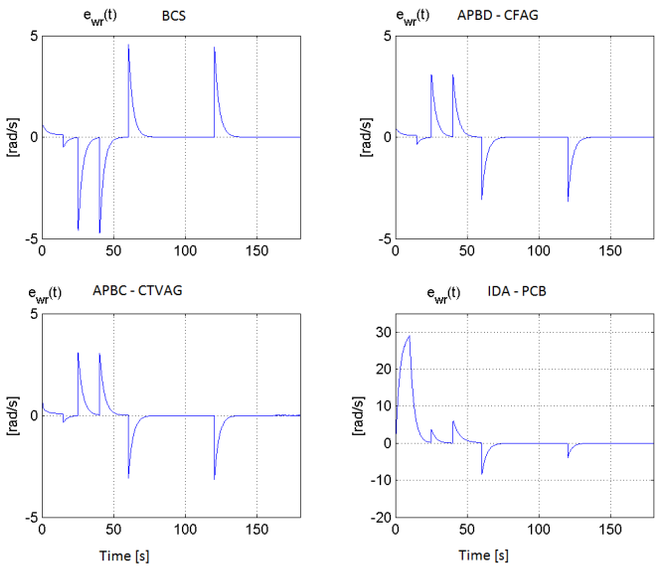

Figure 11. Simulation results for Test 1

The results obtained from Test 1 (Figure 11) show that the smaller errors are obtained by APBC strategies (CFAG and CTVAG) with a maximum error around 3 [rad/s]. This error is less than those obtained from the BCS and the IDA-PBC strategies which are around 5 and 30 [rad/s] respectively. However, the settling time of all four strategies is similar.

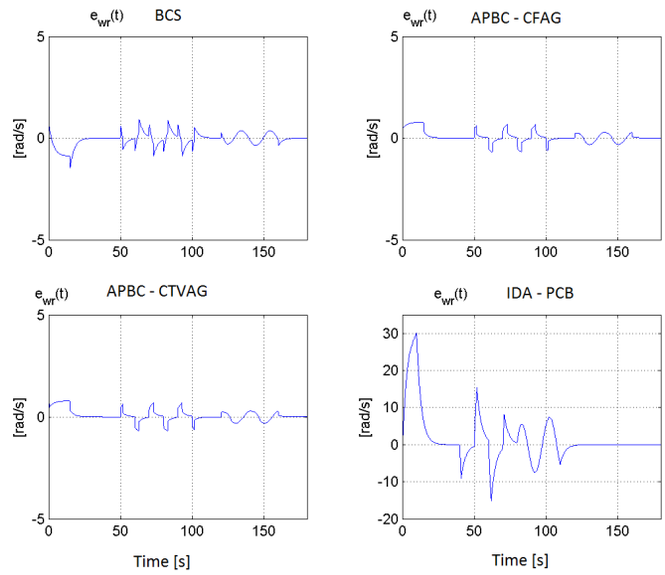

Figure 12. Simulation results for Test 2

From the results obtained for Test 2 (Figure12) a faster stabilization is obtained by the APBC strategies (CFAG and CTVAG), followed by the BCS strategy which was better than the IDA-PBC. The later is strongly dependant on the dynamics of the external loop introduced for controlling the mechanical torque.

3.4. Experimental results using IDA-PBC

In this section the experimental results obtained by applying APBC (CFAG and CTVAG) described in Figure 2 and IDA-PBC strategies described in Figure 10, are presented and compared with the BCS described in Figure 3. The experimental set up as well as the tests carried out for each strategy are described in what follows.

The three phase inverter used in the experiments was that designed and built by González (2005). Communication to PC was done though the software Matlab-Simulink using a customized S-Function. The IM used in the experiments was a Siemens 1LA7080, 0.55KW, cos(ϕ)=0.82, 220V, 2.5A, 4 poles and 1395RPM. From motor tests (no load and locked rotor) the estimated motor parameters used in the study the following: Rs=14.7Ω, Rr=5.5184Ω, Xs=11.5655Ω, Xr=11.5655Ω and Xm=115.3113Ω.

In order to apply resistive torque on motor axis, the induction motor was mechanically coupled to a continuous current generator, Briggs & Stratton ETEK, having a permanent magnet field. The load to the generator was applied using a cage of discrete resistances connected to generator stator and manually controlled by switches. The magnitudes of the resistances were chosen such that maximum values of induction motor operation were not exceeded under any circumstances. The experimental assembly including the motor-generator group used in the experimental tests is shown in Figures 13 (a) and (b).

Test 1 (Basic Behavior): The speed reference was a ramp starting from zero at t=0 to the nominal speed (146.08 rad/s) in 9s. The load torque was kept constant and equal to the nominal value (100%) during the whole test. Initial conditions (IC) for controller parameters were all set to zero, except for the time-varying gains which were chosen as $\Gamma_1(0) = \Gamma_3(0) = I$, where I is the 2x2 identity matrix.

Test 2 (Tracking): A ramp speed referenced was considered, starting from rest at zero and reaching the nominal speed (146.08 [rad/s]) in 9[s]. Between t=40[s] and t=70[s] a pulse train reference of amplitude $0.1\omega_{r_{nom}}$ and frequency π/10 [rad/s] was added on top of the constant nominal value. Between t=80[s] and t=110[s] a sinusoidal reference of amplitude $0.1\omega_{r_{nom}}$ and frequency π/10 was added on top of the constant nominal value. Additionally, the load torque (proportional to the speed) was kept at 50% of the nominal during the whole test. The IC of the controller parameters were all set to zero, except for time-varying gains initial values that were chosen as $\Gamma_1(0) = \Gamma_3(0) = I$, where I is the 2x2 identity matrix.

Test 3 (Regulation): The speed reference was a ramp starting from rest at zero reaching the nominal value(146.08 [rad/s]) in 9s, where the reference was kept constant. Initial load torque was equals to 0% of the nominal value. Between t=40[s] and t=80[s] a torque perturbation equal to 50% of the nominal value is added.

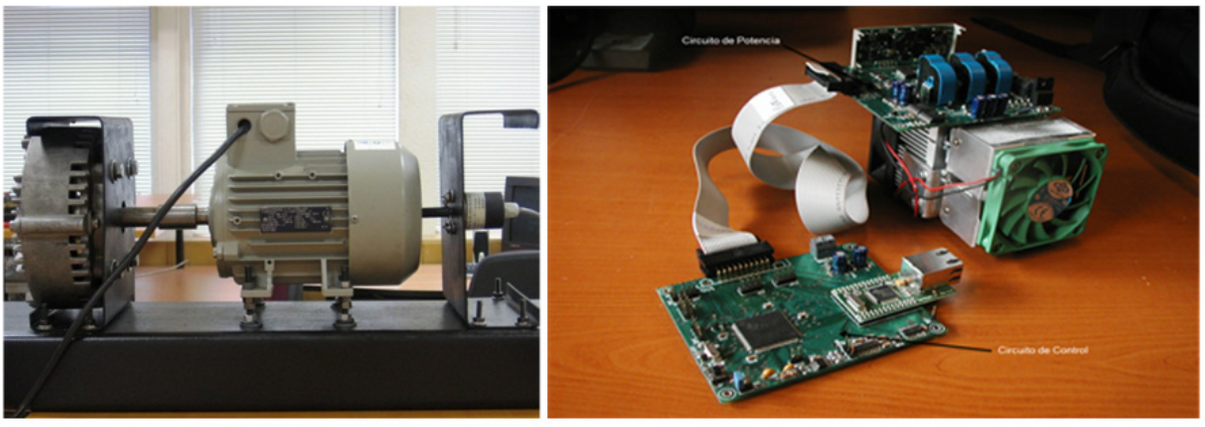

a)

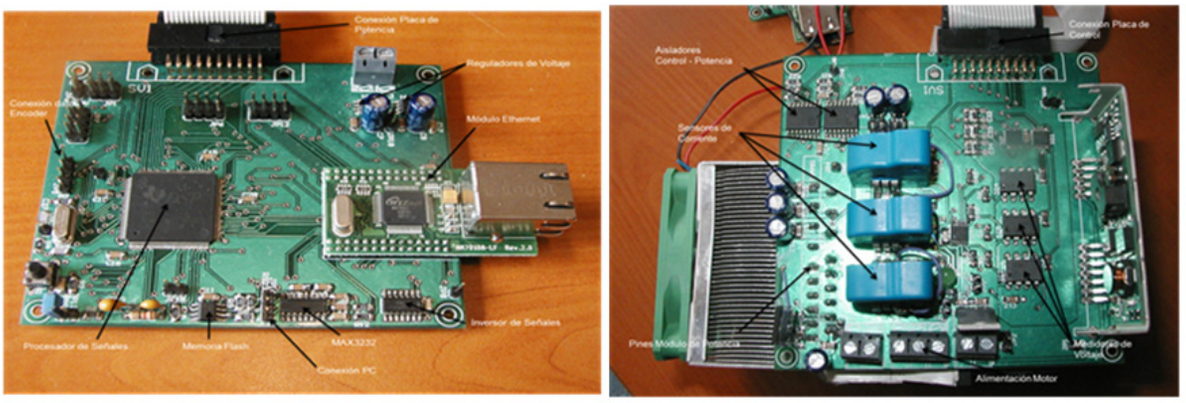

(b)

Figure 13. (a). Experimental assembly. Motor-generator and inverter. (b). Experimental assembly. Control circuit and power circuit.

For the experimental tests, the best values of PI controller parameters for inner and outer loops were chosen based on those obtained from the simulation results of Section 3.2 (González, 2005; González& Duarte-Mermoud, 2005; Pelissier & Duarte-Mermoud, 2007). Later, these values were adjusted during the experiments performing a small number of trial tests. The final values chosen for the constants of control loops used in the BCS and in APBC scheme are as follows: K_P=0.403 and K_I=0.0189 for the outer loop and K_P=45 for the inner loop. For the IDA-PBC strategy, the values of constants k_1 and k_2 were determined based on simulations results reported in Pelissier & Duarte-Mermoud (2007). The chosen values were k_1=k_2=-30 and for the proportional integral loop it K_P=3 and K_I=0.5 were chosen.

For the experimental tests the control strategies were implemented in Matlab/Simulink, using a fixed step of 10[micro s] and the solver ODE5 (Dormand-Prince). In the electronics, a vector modulation with a carrier frequency of 20[kHz] was used. All IC were set to zero except time-varying gains initial values which were chosen as $\Gamma_1(0) = \Gamma_3(0) = I$, where I is the 2x2 identity matrix.

The experimental results obtained after applying the techniques under study for Test 1, Test 2 and Test 3 already described, are shown next. In Figures 14 through 16 the evolution of the speed errors are plotted for each strategy for each one of the tests.

In Figure 14 it is observed the following results: the fastest convergence of control error to zero, with a constant nominal load torque applied (Test 1), was achieved by the IDA-PBC strategy, with about 40[s]. Then 60[s] and 80[s] were obtained by BCS and APBC strategies, respectively. However, in the IDA-PBC strategy an important oscillatory behavior of the control error is observed at the beginning. For more information about the behavior of other variables see González (2005), Pelissier & Duarte-Mermoud (2007) and González et al (2008).

From the tracking viewpoint (Test 2), the best results were achieved for the APBC strategies, which follow reference changes better than the BCS (See Figure 15). The IDA-PBC strategy is not able to follow reference changes properly, presenting an oscillatory behavior of speed error. Convergence of the control error to zero for the IDA-PBC is influenced by rotor flux observer convergence, which necessarily adds a dynamic to the system affecting the global behavior of the overall system. For information about the evolution of other variables see González (2005), Pelissier & Duarte-Mermoud (2007) and González et al (2008).

When applying torque perturbations on the motor axis (Test 3), it is observed that fastest stabilization was attained by APBC strategies, without large oscillations (see Figure 16). The IDA-PBC strategy, although perturbations are quickly controlled, has an oscillatory control error. The BCS case is the slowest with a larger error in stationary state. This last strategy is not robust in the presence of perturbations on the mechanical subsystem. The evolution of other variables can be seen in (González, 2005; Pelissier & Duarte-Mermoud, 2007; González et al., 2008).

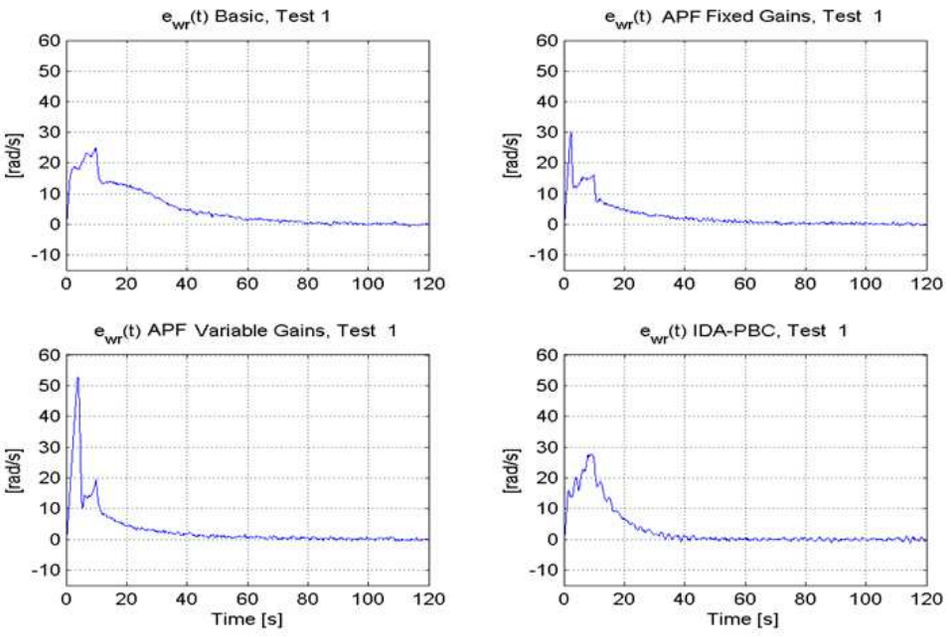

Figure 14. Speed errors for experimental Test 1 with constant load torque

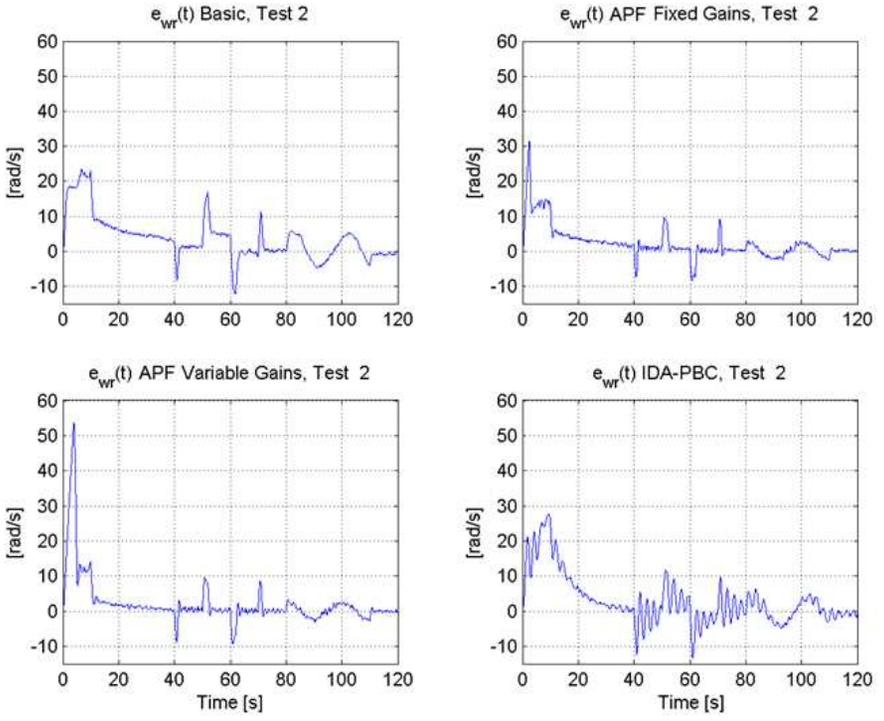

Figure 15. Speed errors for experimental Test 2 for reference tracking

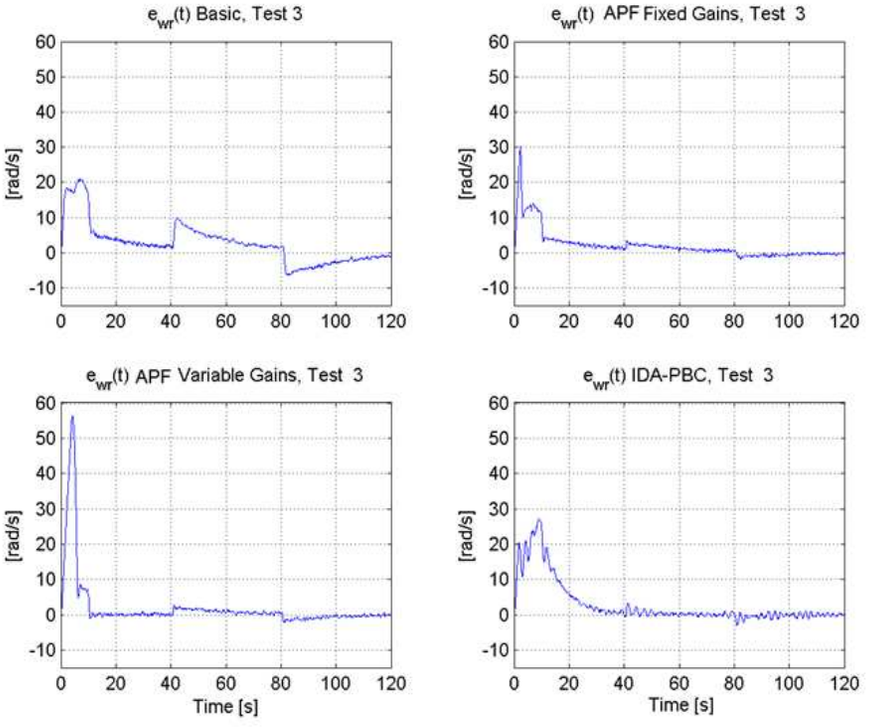

Figure 16. Speed errors for experimental Test 3 for load torque perturbations

Numerous other experiments and simulations, not shown here for the sake of space, were carried out to analyze the influence of several other parameters on the BCS, APBC and IDA-

PBC strategies (Travieso, 2002; Pelisssier, 2006). In particular the effects of initial conditions on APBC strategies, as well as the effects of using fixed and time-varying adaptive gains were analyzed. It was observed, in general, that time-varying gains improve transient behavior and diminish initial control error. In simulations, a small noise was added on these signals and the performance of the method were not affected significantly (González, 2005). At the experimental level, the influence of the normal noise present in the measurement of current signals during the test did not affect the behavior of the APBC. For higher noise levels some deterioration of the control system behavior was observed. In this case, more robust adaptive laws should be used. For instance the σθ-modification (Narendra & Annaswamy, 1989) could be used.

4. Induction motor speed control using fractional order PI controllers

In this section we present a field oriented control scheme like the one shown in Figure 2, where the PI controller used in the speed loop is changed to a PI controller in which the integral order is not unity (fractional integral effect). The main idea to explore is that fractional order integrals are of benefit in this kind of IM controllers.

4.1. Fractional order PI controllers

The FOPI controller is based on the same principles as the classical PI controller, with the difference that in this case the control action is calculated by means of fractional order integrals. The transfer function of a FOPI controller is given by

$$H_{FOPI}(s) = k_p + k_i / s^{\nu} \tag{25}$$

where ν denotes the integration order, k_p is the proportional constant and k_i is the integral constant. The detailed computation of fractional integrals is shown (Valério, 2005). Expression (8) allows computing fractional integrals $\nu < 0$ and fractional derivatives $\nu > 0$, corresponding to Caputo's definition (Oldham & Spanier, 1974; Kilbas et al., 2006; Sabatier et al., 2007).

$$\frac{d^{\nu}}{dx^{\nu}} = \begin{cases} \dfrac{1}{\Gamma(-\nu)} \displaystyle\int_{x_0}^{x} (x-t)^{-\nu-1} f(t)dt, & \nu < 0 \\ f(x), & \nu = 0 \\ \dfrac{1}{\Gamma(-\nu)} \displaystyle\int_{x_0}^{x} (x-t)^{-\nu-1} \left[D^m f(t) \right] dt, & \nu > 0 \end{cases} \tag{26}$$

In this equation x corresponds to the integration variable, Γ corresponds to Gamma function, m denotes the integer immediately greater than ν, and D denotes the integer derivative with respect to x. The Laplace Transform of fractional order derivatives and integrals (according to Caputo's definition) is shown in (9), where $F(s) = \mathcal{L}\{f(x)\}$.

$$L\left\{\frac{d^{\nu}}{dx^{\nu}}f(x)\right\}=\begin{cases} s^{\nu}F(s), & \nu \le 0 \\ s^{\nu}F(s)-\sum_{k=0}^{n-1}s^{k}\left({}_{0}^{x}D^{\nu-k-1}\right)f(0), & \nu > 0 \end{cases} \tag{27}$$

Other definitions commonly used in fractional calculus can be found in Oldham & Spanier (1974), Valério (2005), Kilbas et al (2006) and Sabatier et al (2007).

In this study the FOC scheme shown in Figure 2 (changing the PI controllers by FOPI controllers in the spped control block) is used to control the speed of an IM. The "Speed Controller" block shown in Figure 2 corresponds to a FOPI controller, in which the parameter ν will be modified to analyze its effects on the controlled system. This strategy will be denoted as FOC-FOPI and will be compared with the classical strategy using a standard PI controller (BCS), which will be denoted as FOC-PI. Notice that this case corresponds to the FOC-FOPI strategy when $\nu = 1$. "Current Controller" block and "Flux Controller" block in Figure 2 correspond to proportional controllers. All these controller parameters (proportional constants) will be kept constant at values indicated in Section 4.2.

4.2. Simulation set up

The controlled system corresponds to the Siemens 3-phase IM, model 1LA7080 descrbed in Section 3.3. All the simulations shown in this study were performed using MATLAB/Simulink. The following describes the tests performed on the IM, in simulation analysis. These tests were used to determine the general features of FOC-FOPI scheme, and will be compared with FOC-PI scheme. For the sake of space only results concerning the regulation of the controlled system (capacity of the system reject external perturbations at different levels of load) are shown. Although the tracking study (capacity of the system to reach and follow a pre-specified speed reference at different levels of load) was also done (Mira, 2008; Mira & Duarte-Mermoud, 2009; Duarte-Mermoud et al, 2009) the simulated results are not shown here.The simulation results will be analyzed and discussed including stabilization time, rise time and control effort, among other aspects.

Test 1(Regulation): The speed reference increases from zero at a rate of 16 $[rad/s^2]$) until nominal speed ($146.08[rad/s] = 1395[rpm]$) in $9.33[s]$. Then the reference is kept constant at the nominal speed until the end of the test ($315[s]$). (See Figure 4). The mechanical load varies during the test as shown in Table 2 and Figure 17.

The FOPI controller has the transfer function shown in (7). In all tests, parameters k_p and k_i were kept fixed at 0.5 and 0.05 respectively. These values were chosen after performing a series of preliminary simulation tests, analyzing the stabilization time and the control effort for different values. The values of the proportional constant used in current and flux proportional controllers were chosen to be 45. This value was also determined after a series of preliminary tests. The integration order was changed to explore the system's sensitivity with respect to parameter ν. The results shown in the next section include orders 0.7, 1.0 (Classical PI), 1.7 and 2.0. Theoretically the limit of stability is at ν = 2, a fact verified at the

simulation level (Mira & Duarte-Mermoud, 2009). See also Figure 21. Many other integration orders have been analyzed at the simulation level but they are not shown here for the sake of space. The reader is referred to Mira (2008) for more details.

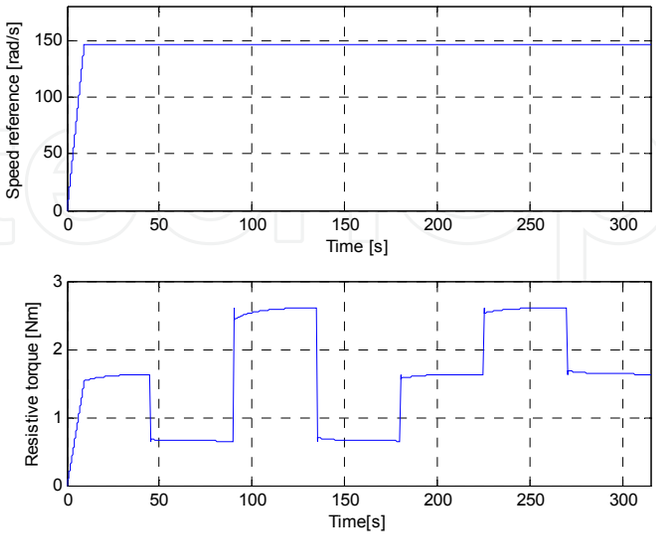

Figure 17. Description of Test 1 (Regulation)

Interval [s]	Level of load
0 – 45	50%
45 – 90	0%
90 – 135	100%
135 – 180	0%
180 – 225	50%
225 – 270	100%
270 – 315	50%

Table 1. Variation of load torque

4.3. Simulation results (regulation)

In this section the simulated behavior of IM control under the FOC-FOPI scheme, when Test 1 is applied, is shown in Figs. 18 to 21, for different values of the integration order ν of the integral part of PI controller (ν = 0.7, ν = 1.0, ν = 1.7 and ν = 2.0). Note that the classical FOC-PI scheme is obtained from the FOC-FOPI strategy by setting ν = 1. In all the figures, only the controlled variable (motor speed) is shown. The results obtained are quite satisfactory, as can be seen from Figures 18 to 21. The evolution of the controlled variable tries to follow the speed reference at all times, in spite of the perturbation being applied.

From Figure 18 it can be observed that for integration orders less than 1.0 the response presents no overshoot although the response is slower. It can be concluded, from information contained in Figure 20, that the response is faster when the integration order is greater than 1.0 but an overshoot is observed. When ν is chosen as 2.0 critically stable behavior is attained, as shown in Figure 21

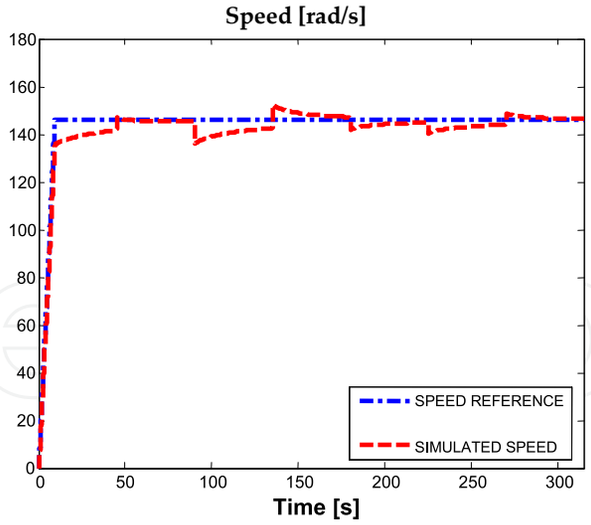

Figure 18. Simulation results for $\nu = 0.70$

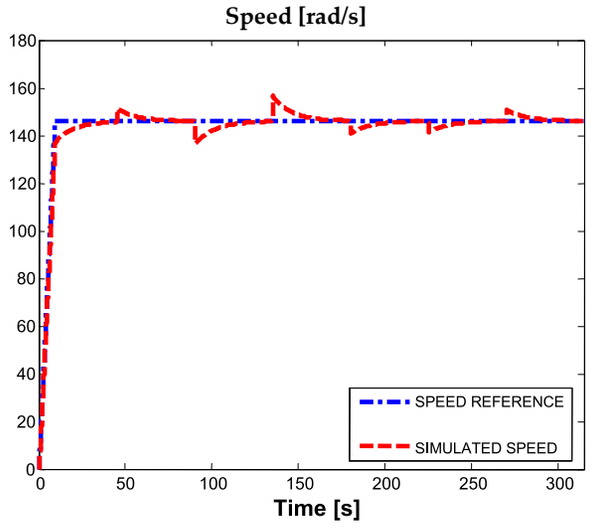

Figure 19. Simulation results for $\nu = 1.00$

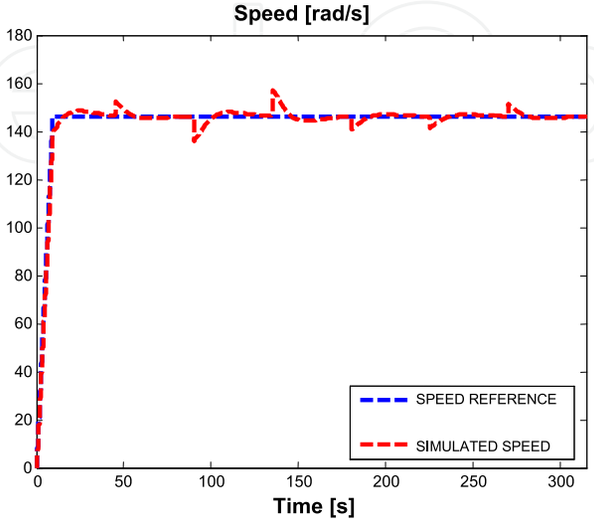

Figure 20. Simulation results for $\nu = 2.00$

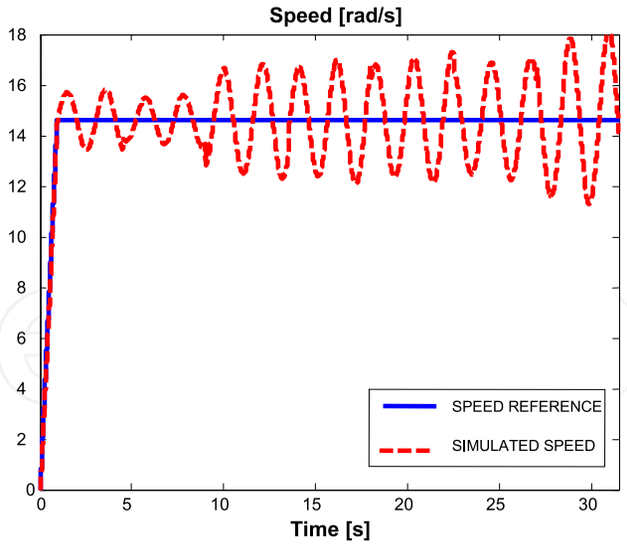

Figure 21. Simulation results for $\nu = 1.30$

Experimental analysis of the FOC-FOPI scheme is currently underway. These results will be reported, compared and discussed in the near future.

5. Conclusions

From simulation and experimental analysis performed on induction motor control some interesting conclusions can be drawn. In APBC strategies an important simplification of control scheme based on FOC principle can be attained when using the TFCP, allowing an effective control of the system without the necessity of having a rotor flux sensor or implementing a rotor flux observer to orientate the field. For APBC strategy the use of time-varying adaptive gains noticeably improves the transient behavior of controlled system, both for tracking as well as for regulation, when compared with the APBC strategy with fixed adaptive gains and also when compared with classical control strategies. Results are very similar for both the SISO and the MIMO approaches when using APBC. Compared with other control schemes proposed in the literature such as those based on traditional PI (Chee-Mun, 19998), sliding modes (Chan & Wang, 1996 ; Dunningan et al, 1998 ; Taoutaou & Castro-Linares, 2000; Araujo & Freitas, 2000), artificial intelligence (Bose, 1997 ; Vas, 1999) and non adaptive passivity (Taoutaou & Castro-Linares, 2000; Espinosa & Ortega, 1995), we have been able to develop four simple and novel controllers. They have adaptive characteristics, being robust in the presence of load parameter variations. Simple proportional controllers are used for the rotor speed, rotor flux and stator current control loops. They are also robust for a large range of proportional gain variations.

In the case of energy shaping strategy, IDA-PBC, a novel control scheme was studied and implemented. Since the original strategy was only designed for speed control, the addition of an outer speed loop of proportional-integral type, allowed obtaining certain robustness with respect to torque perturbations. In this strategy was necessary the design and implementation of a rotor flux observer, adding certain complexity to the complete system.

Since the BCS has fixed controller parameters its behavior is not as good as the adaptive strategies studied and presented here.

From simulation results obtained in this study it is possible to state that the integration order of FOPI controller plays a central role in speed control of an IM, when compared with the BCS. Choosing a suitable value of the integration order allows obtaining fast/slow responses and over/under damped responses. For this particular case of IM speed control , it was observed that for integration orders lesser than 1 the stabilization time is rather large and the controlled variable may not present overshoot. On the contrary, for values over 1 the stabilization time is small (and diminishes as integration order increases); the overshoot increases as the integration order does, reaching instability for integration order equal to 2. It was observed that the best results obtained from this study correspond to integration orders near to 1.40, presenting small rise and stabilization times, though with certain degree of overshoot.

In conclusion, the adaptive strategies studied present clear advantages with respect to the BCS used as basis of comparison. Amongst the adaptive schemes the APBC with time-varying adaptive gains is the one that behaves better.

Author details

Manuel A. Duarte-Mermoud & Juan C. Travieso-Torres
Department of Electrical Engineering, University of Chile, Santiago, Chile

Acknowledgement

The results reported here have been supported by CONICYT-Chile under grants Fondecyt 1061170, Fondecyt 1090208 and FONDEF D05I-10098.

6. References

Al-Nimma, D.A. and Williams, S. (1980). Study of rapid speed-changing methods on A.C. motor drives. *IEE Proceedings, Part B, Electric Power Applications*, Vol.127, No.6, pp. 382 – 385, ISSN: 0143-7038

Araujo, R. E. & Freitas, D. (2000), "Non-linear control of an induction motor : sliding mode theory leads to robust and simple solution ". *International Journal of Adaptive Control and Signal Processing*, Vol.14, No. 2, pp. 331-353, MES, ISSN: 0890-6327.

Bose, B.K. (1997). *Power Electronics and Variable Frequency Drives; Technology and Applications*. IEEE Press Marketing, ISBN-13: 978-0780310841, New York, USA

Bose, B.K. (2002). *Modern Power Electronics and AC Drives*, Prentice Hall PTR, ISBN-13: 978-0130167439, Upper Saddle River, USA

Byrnes, C.I., Isidori, A. & Willems, J.C. (1991), "Passivity, feedback equivalence, and the global stabilization of minimum phase nonlinear systems". *IEEE Transactions on Automatic Control*, Vol. 36, No. 11, pp. 1228-1240, November, ISSN: 0018-9286.

Castro-Linares, R. & Duarte-Mermoud, M.A. (1998), "Passivity equivalence of a class of SISO nonlinear systems via adaptive feedback". *Proceedings of VIII Latinamerican Congress on Automatic Control*, 9 – 13 November, Vol. 1, pp. 249-254.

Chan, C.C. & Wang, H.Q. (1996), "New scheme of sliding-mode control for high performance induction motor drives". *IEE Proceedings on Electrical Power Applications*, Vol. 143, pp. 177-185, ISSN: 1350-2352.

Chee-Mun, O. (1998), *Dynamic Simulation of Electric Machinery, using Matlab/Simulink*. Prentice Hall PTR, ISBN-10: 0137237855, ISBN-13: 978-0137237852, USA.

Duarte-Mermoud M.A., Castro-Linares R. and Castillo-Facuse A. (2001), "Adaptive passivity of nonlinear systems using time-varying gains". *Dynamics and Control*, Vol. 11, No. 4, December, pp. 333-351, ISSN: 0925-4668.

Duarte-Mermoud, M.A. & Travieso-Torres, J.C. (2003), "Control of induction motors: An adaptive passivity MIMO perspective". *International Journal of Adaptive Control and Signal Processing*, Vol. 17, No. 4, May, pp. 313-332, ISSN: 0890-6327.

Duarte-Mermoud, M.A., Castro-Linares, R. & Castillo-Facuse, A. (2002), "Direct passivity of a class of MIMO nonlinear systems using adaptive feedback". *International Journal of Control*. Vol.75, No. 1, January, pp. 23-33, ISSN: 0020-7179.

Duarte-Mermoud, M.A., Méndez-Miquel, J.M., Castro-Linares, R. & Castillo-Facuse, A. (2003), "Adaptive passivation with time-varying gains of MIMO nonlinear systems". *Kybernetes*, Vol. 32, Nos. 9/10, pp. 1342-1368, ISSN: 0368-492X.

Duarte-Mermoud, M.A., Mira, F.J., Pelissier, I.S. & Travieso-Torres, J.C., "Evaluation of a fractional order PI controller applied to induction motor speed Control". *Proceedings of the 8th IEEE International Conference on Control & Automation (ICCA2010)*, June 9-11, 2010, Xiamen, China. Proc. in CD, Paper No. 790, ThA4.5, ISBN: 978-1-4244-5195-1.

Dunnigan, M.W., Wade, S., Williams, B.W. & Yu, X. (1998), "Position control of a vector controlled induction machine using Slotine's sliding mode control approach". *IEE Proceedings on Electrical Power Applications*, Vol. 145, pp. 231-248, ISSN: 1350-2352.

Espinosa, G. and Ortega, R. (1995), "An output feedback globally stable controller for induction motors". *IEEE Transaction on Automatic Control*, Vol. 40, pp. 138-143, ISSN: 0018-9286.

González, H. (2005). *Development of Control Schemes based on Energy Shaping for a Class of Nonlinear Systems and Design of an Open Three Phase Inverter for on-line Applications in Induction Motors*. (In Spanish). M.Sc. Thesis, Department of Electrical Engineering, University of Chile

González, H., Duarte-Mermoud, M.A., Pelissier, I., Travieso J.C. & Ortega, R. (2008). A novel induction motor control scheme using IDA-PBC. *Journal of Control Theory and Applications*. Vol. 6, No. 1, January 2008, pp. 123-132, ISSN: 1993-0623.

González, H.A. & Duarte-Mermoud, M.A. (2005a). Induction motor speed control using IDA-PCB". (In Spanish). *Anales del Instituto de Ingenieros de Chile (Annals of the Chilean Institute of Engineers)*, Vol.117, No.3, December 2005, pp. 81-90 ISSN 0716-3290.

Isidori, A. (1995), *Nonlinear Control Systems*. Springer Verlag, Third Ed, ISBN-10: 3540199160, ISBN-13: 978-3540199168, USA.

Jansen, P.L.; Lorenz, D. & Thompson, C.O. (1995). Observer-based direct field orientation for both zero and very high speed operation. *IEEE Ind. Applic. Society Magazine*, Vol.1, No.4, (Jul. 1995), pp. 7-13, ISSN 1077-2618.

Kilbas, A. A.; Srivastava, H. M. & Trujillo, J. J. (2006). *Theory and Applications of Fractional Differential Equations.* Elsevier Science Inc., North-Holland Mathematics Studies, Vol.204, ISBN 978-0-444-51832-3, New York, USA

Marino, R.; Peresada, S. & Tomei, P. (1994). Adaptive observers for induction motors with unknown rotor resistance. *Proceeding of the 33rd Conf. on Decision and Control*, Vol.1, pp. 4018-4023, ISBN 0-7803-1968-0, Orlando, Florida, USA, December 1994

Martin, C. (2005). *A Comparative Analysis on Magnetic Flux Observers for Induction Motor Control Schemes*. (In Spanish). E.E. Thesis, Department of Electrical Engineering, University of Chile

Mira, F. (2008). *Design of a Three Phase Inverter and its Application to Advanced Control of Electrical Machines*. (In Spanish), E. E. Thesis, Dept. Elect. Eng., University of Chile

Mira, F.J. & Duarte-Mermoud, M.A. (2009). "Speed control of an asynchronous motor using a field oriented control scheme together with a fractional order PI controller. (In Spanish). *Annals of the Chilean Institute of Engineers*, Vol.121, No.1, pp. 1-13, ISSN 0716-3290.

Narendra, K.S. & Annaswamy, A.S. (1989). *Stable Adaptive Systems*. Prentice Hall, ISBN 0-13-839994-8, Englewood Cliffs, New Jersey, USA

Nijmeijer, H. & Van der Schaft, A. (1990), *Nonlinear Dynamical Control Systems*. Springer Verlag, ISBN-10: 038797234X, ISBN-13: 978-0387972343, USA.

Oldham, K. B. & Spanier, J. (1974). *The Fractional Calculus: Theory and Applications of Differentiation and Integration to Arbitrary Order.* Academic Press, Inc., Mathematics in Science and Engineering, Vol.111, ISBN 0-12-558840-2, New York, USA.

Ortega, R. & García-Canseco, E. (2004). Interconnection and damping assignment passivity-based control: A survey. *European Journal of Control*, Vol.10, No.5, pp. 432-450, ISSN 0947-3580.

Ortega, R., van der Schaft, A., Maschke, B. & Escobar, G. (2002). Interconnection and damping assignment passivity-based control of port-controlled Hamiltonian systems. *Automatica*, Vol.38, pp. 585-596, ISSN 0005-1098.

Pelissier, I. & Duarte-Mermoud, M.A. (2007). Simulation comparison of induction motor schemes based on adaptive passivity and energy shaping. (In Spanish). *Anales del Instituto de Ingenieros de Chile (Annals of the Chilean Institute of Engineers)*, Vol.119, No.2, August 2007, pp. 33-42, ISSN 0716-3290.

Pelissier, I. (2006). *Advanced strategies for induction motor control*. (In Spanish). E.E. Thesis, Department of Electrical Engineering, University of Chile

Sabatier, J.; Agrawal, O. P. & Machado, J. A. Eds. (2007). *Advances in Fractional Calculus: Theoretical Developments and Applications in Physics and Engineering.* Springer Verlag, ISBN ISBN 978-90-481-7513-0, New York, USA.

Taoutaou, D. & Castro-Linares, R. (2000), "A controller-observer scheme for induction motors based on passivity feedback equivalence and sliding modes". *International Journal of Adaptive Control and Signal Processing*, Vol. 14, No. 2-3, pp. 355-376, ISSN: 0890-6327.

Travieso, J.C. (2002). *Passive equivalence of induction motors for control purposes by means of adaptive feedback*. (In Spanish). Ph.D. Thesis, Electrical Engineering Department, Universidad de Santiago de Chile

Travieso-Torres, J.C. & Duarte-Mermoud, M.A. (2008), "Two simple and novel SISO controllers for induction motors based on adaptive passivity". *ISA Transactions*, Vol. 47, No. 1, January, pp.60-79, ISSN 0019-0578.

Valério, D. (2005). *Fractional Robust System Control.* Ph.D. Dissertation, Instituto Superior Técnico, Universidade Técnica de Lisboa, Portugal

Van der Schaft, A. (2000). *L2-Gain and Passivity Techniques in Nonlinear Control*. 2nd Edition. Springer-Verlag, ISBN: 1-85233-073-2, London, GB

Vas, P. (1998). *Sensorless Vector and Direct Torque Control.* Oxford University Press, ISBN-10: 0198564651, N-13: 978-0198564652, New York, USA

Vas, P. (1999). *Artificial-Intelligence-Based Electrical Machines and Drives*. Oxford University Press, ISBN-10: 019859397X, ISBN-13: 978-0198593973, USA.

Williams, B.W. & Green, T.C. (1991). Steady state control of an induction motor by estimation of stator flux magnitude. *IEE Proceedings, Part B, Electric Power Applications*, Vol.138, No.2, pp. 69 -74, ISSN: 0143-7038